Table 3. Correlation between NS5A and core protein polymorphisms and on-treatment virological responses of patients treated with PEG-IFN/RBV

Protein	Factor	Total†	RVR‡	Non-RVR	EVR	Non-EVR	ETR	Non-ETR	*P* value: RVR vs non-RVR	*P* value: EVR vs non-EVR	*P* value: ETR versus non-ETR
NS5A	IRRDR ≥ 4	40	8 (20%)	32 (80%)	30 (75%)	10 (25%)	33 (83%)	7 (17%)	**0.047**	**0.005**	**0.02**
	IRRDR ≤ 3	17	0 (0.0%)	17 (100%)	6 (35%)	11 (65%)	9 (53%)	8 (47%)			
	ISDR ≥ 1	31	5 (16%)	26 (84%)	24 (77%)	7 (23%)	26 (84%)	5 (16%)	0.62	**0.01**	0.057
	ISDR = 0	26	3 (12%)	23 (88%)	12 (46%)	14 (54%)	16 (62%)	10 (38%)			
Core	Wild-core (Arg^{70}/Leu^{91})	24	4 (17%)	20 (83%)	17 (71%)	7 (29%)	19 (79%)	5 (21%)	0.63	0.31	0.42
	Non-wild-core	33	4 (12%)	29 (88%)	19 (58%)	14 (42%)	23 (70%)	10 (30%)			
	Gln^{70}	14	2 (14%)	12 (86%)	4 (29%)	10 (71%)	5 (36%)	9 (64%)	0.97	**0.002**	**0.0002**
	Non- Gln^{70}	43	6 (14%)	37 (86%)	32 (74%)	11 (26%)	37 (86%)	6 (14%)			
	Met^{91}	22	1 (5%)	21 (95%)	12 (54%)	10 (46%)	16 (73%)	6 (27%)	0.1	0.29	0.9
	Non- Met^{91}	35	7 (20%)	28 (80%)	24 (69%)	11 (31%)	26 (74%)	9 (26%)			

†, total number of isolates with a given factor; ‡, number of RVR, non-RVR, EVR, non-EVR, ETR or non-ETR cases with a given factor. *P* values indicating statistically significant difference are written in bold.

Table 4. Correlation between IRRDR polymorphism and patients' demographic characteristics

Factor	IRRDR ≥ 4	IRRDR ≤ 3	*P* value
Age	54.1 ± 9.5†	59.2 ± 6.9	**0.035**
Sex (male/female)	23/17	11/6	0.61
Body weight (Kg)	62.4 ± 18.8	64.2 ± 12.1	0.68
Platelets (× $10^4/mm^3$)	17.0 ± 5.0	17.7 ± 5.0	0.66
Hemoglobin (g/dl)	14.3 ± 1.2	14.7 ± 1.1	0.21
Neutrophil count	2303 ± 822	2432 ± 658	0.57
γ-GTP (IU/L)	52.6 ± 42.3	80.7 ± 70.5	0.15
Glutamate pyruvate transaminase (IU/L)	80.2 ± 60.7	101.6 ± 79.7	0.33
HCV-RNA (KIU/mL)	1719 ± 1298	2273 ± 1571	0.21

†, mean ± S.D. *P* values indicating statistically significant difference are written in bold.

either a non-SVR or null-response (Table 2 and Fig. 2). Gln^{70} was also the only factor of core protein that was strongly associated with non-EVR and non-ETR responses (Table 3).

Identification of independent viral factors that are significantly correlated with virological responses to pegylated-interferon/ribavirin therapy

In order to identify which independent viral factors are significantly correlated with final and on-treatment responses to PEG-IFN/RBV therapy, data including all available baseline patient variables, NS5A and core polymorphic factors, and previously published data on polymorphism in an N-terminus of NS3 of the same patient cohort (16) were analyzed by univariate and multivariate logistic regression analyses (Table 5). In regard to the final treatment responses, IRRDR ≥ 4 and group A of the N-terminus of NS3 were identified as independent viral factors that are significantly associated with a SVR, whereas IRRDR ≤ 3 and Gln^{70} of core were identified as independent factors associated with a null response. Regarding on-treatment responses, IRRDR ≥ 4 and non-Gln^{70} were identified as independent factors associated with an EVR and ETR.

DISCUSSION

Pegylated-interferon/ribavirin combination therapy has been used to treat chronic HCV infection, the treatment outcome being thought to be affected by both host and viral factors. Recently, IL28B, which encodes IFNλ3, was identified as the major host factor that determines the treatment outcome (22–24). As for the viral factor(s), we and other research groups have reported that

Table 5. Univariate and multivariate logistic regression analyses to identify independent factors significantly associated with virological responses to PEG-IFN/RBV therapy

	Univariate		Multivariate	
Response	Variable	*P* value	Odds ratio (95% CI)	*P* value
SVR	**IRRDR ≥ 4**	0.003	5.2 (1.3–20.1)	**0.02**
	ISDR ≥ 1	0.013		
	Non-Gln^{70}	0.016		
	NS3 / A group	0.013	4.2 (1.0–18.3)	**0.05**
	Viral load	0.04		
Null response	**IRRDR ≤ 3**	0.001	0.2 (0.04–0.7)	**0.02**
	ISDR = 0	0.06		
	Gln^{70}	0.0001	7.8 (1.7–35.5)	**0.008**
	Viral load	0.08		
	NS3 / non-A group	0.03		
	Hemoglobin	0.02		
	γ-GTP	0.08		
Relapse	**Age**	0.02	1.2 (1.0–1.3)	**0.03**
	Sex	0.004		
	Hemoglobin	0.03		
RVR	IRRDR ≥ 4	0.05		
	Hemoglobin	0.02	0.4 (0.2–0.9)	**0.03**
EVR	**IRRDR ≥ 4**	0.001	7.0 (1.6–29.8)	**0.009**
	ISDR≥1	0.01		
	Non-Gln^{70}	0.002	0.2 (0.04–0.8)	**0.02**
	NS3 / A group	0.07		
	Viral load	0.015		
	Hemoglobin	0.07		
	γ-GTP	0.09		
ETR	**IRRDR≥4**	0.001	6.2 (1.4–27.7)	**0.02**
	ISDR≥1	0.06		
	Non-Gln^{70}	0.0001	0.1 (0.03–0.6)	**0.008**
	NS3 / A group	0.03		
	Viral load	0.08		
	Hemoglobin	0.02		
	γ-GTP	0.08		

Variables that were shown by multivariate analysis to be significantly correlated with a certain treatment response are written in bold.

heterogeneity of NS5A and the core proteins of HCV-1b are correlated with treatment outcome (11–15). Furthermore, we recently reported that polymorphism in an N-terminus of NS3 is significantly correlated with virological responses to PEG-IFN/RBV therapy (16). In the present study, we have further expanded the previous study by analyzing possible correlations between heterogeneity of NS5A and the core regions of the HCV-1b genome and virological responses to PEG-IFN/RBV therapy. The present study showed that final and on-treatment responses of patients in the same cohort were also significantly influenced by IRRDR ≥ 4, ISDR ≥ 1 of NS5A, and Gln^{70} of the core protein.

We previously reported IRRDR ≥ 6 as an independent viral factor significantly associated with SVR in different patient cohorts in Hyogo Prefecture (11, 15). Also, ISDR ≥ 2 was identified as the optimal threshold for SVR prediction (20, 25–27). However, in the present study IRRDR ≥ 6 or ISDR ≥ 2 did not correlate significantly with a SVR, although there was a trend toward SVR in these criteria (11 of 16 isolates with IRRDR ≥ 6 and 8 of 11 isolates with ISDR ≥ 2 were obtained from SVR patients). This difference might be attributable to the low prevalence of IRRDR ≥ 6 (16/57) and ISDR ≥ 2 (13/57) in the present patient cohort. Accordingly, in this study the IRRDR and ISDR sequences of the HCV isolates were less variable than were those of other studies. It thus appears that the prevalence of HCV isolates of IRRDR ≥ 6 and ISDR ≥ 2 varies from one geographical region to another. This implies the possibility that certain characteristics of HCV isolates, including IFN sensitivity, may also vary from one geographical region to another. Analysis in a large-scale multicenter study is needed to clarify this possibility.

The NS5A- interferon sensitivity-determining region was first identified to be significantly correlated with the probability of a SVR during the era of IFN monotherapy (10). In the more recent era of combination therapy with PEG-IFN/RBV, the NS5A-IRRDR has been identified to be closely associated with a SVR (11). The ISDR interacts with PKR and regulates replication of HCV *in vitro* (28). Mutations in the ISDR affect the interaction with PKR and may inhibit viral replication. In the case of the IRRDR, the molecular mechanism underlying the possible involvement of this region in IFN responsiveness of the virus is still unknown. The significant difference among IRRDR sequence patterns may suggest genetic flexibility of this region. Thus, changes in the IRRDR might be capable of modulating intracellular antiviral activity, or maybe the genetic flexibility of this region is accompanied by compensatory changes elsewhere in the viral genome and these compensatory changes affect overall viral fitness and responses to IFN therapy (29–31)

When we investigated the impact of various sequences patterns at positions 70 and 91 of the core protein, we observed that single point mutation at position 70 (Gln^{70} vs non-Gln^{70}) was the only factor that significantly influenced treatment responses. This result is consistent with recent reports, including a recent multi-center study in Japan that identified Gln^{70} as a predictive factor for poor responses to PEG-IFN/RBV treatment (14, 13, 30). The core region of HCV interacts with several host factors and modulates expression of numerous genes, including down-regulating IFN-induced antiviral genes, thus inhibiting the antiviral action of IFN (32, 33). Therefore, it would also be interesting to investigate the impact of

polymorphism, both at position 70 and of NS5A, on HCV pathogenesis and IFN sensitivity.

Multivariate logistic regression analysis of all available data, including those of NS5A and core polymorphisms in this study and the data on NS3 polymorphism in the same patient cohort published elsewhere (16), identified IRRDR $\geq$ 4 and group A of NS3 as independent viral factors that are significantly associated with a SVR, and IRRDR $\leq$ 3, and Gln^{70} of the core protein as independent factors significantly associated with a null response (Table 5). No combinations of these criteria produced a more significant correlation with virological responses to PEG-IFN/RBV therapy (data not shown).

In conclusion, the present results demonstrate that sequence heterogeneity of NS5A, especially in IRRDR and ISDR, and a single-point mutation at position 70 of the core protein of HCV-1b are significantly correlated with virological responses to PEG-IFN/RBV therapy. Also, the results emphasize the possible functional importance of NS5A and core protein in regulating viral responsiveness to PEG-IFN/RBV.

ACKNOWLEGMENTS

This study was supported in part by Health and Labor Sciences Research Grants from the Ministry of Health, Labor and Welfare, Japan, and a Science and Technology Research Partnership for Sustainable Development grant from the Japan Science and Technology Agency and Japan International Cooperation Agency. This study was also carried out as part of the Japan Initiative for Global Research Network on Infectious Diseases, Ministry of Education, Culture, Sports, Science and Technology, Japan, and the Global Center of Excellence Program at Kobe University Graduate School of Medicine.

REFERENCES

1. Amoroso P., Rapicetta M., Tosti M.E., Mele A., Spada E., Buonocore S., Lettieri G., Pierri P., Chionne P., Ciccaglione A.R., Sagliocca L. (1998) Correlation between virus genotype and chronicity rate in acute hepatitis C. *J Hepatol* **28**: 939–44.
2. Tanaka E., Kiyosawa K. (2000) Natural history of acute hepatitis C. *J Gastroenterol Hepatol* **15**(Suppl): E97–104.
3. Maekawa S., Enomoto N. (2009) Viral factors influencing the response to the combination therapy of peginterferon plus ribavirin in chronic hepatitis C. *J Gastroenterol* **44**: 1009–15.
4. Mattsson L., Sonnerborg A., Weiland O. (1993) Outcome of acute symptomatic non-A, non-B hepatitis: a 13-year follow-up study of hepatitis C virus markers. *Liver* **13**: 274–8.
5. Micallef J.M., Kaldor J.M., Dore G.J. (2006) Spontaneous viral clearance following acute hepatitis C infection: a systematic review of longitudinal studies. *J Viral Hepat* **13**: 34–41.
6. Fried M.W., Shiffman M.L., Reddy K.R., Smith C., Marinos G., Goncales F.L. Jr., Haussinger D., Diago M., Carosi G., Dhumeaux D., Craxi A., Lin A., Hoffman J., Yu J. (2002) Peginterferon alfa-2a plus ribavirin for chronic hepatitis C virus infection. *N Engl J Med* **347**: 975–82.
7. Sarasin-Filipowicz M. (2009) Interferon therapy of hepatitis C: molecular insights into success and failure. *Swiss Med Wkly* **140**: 3–11
8. Backus L.I., Boothroyd D.B., Phillips B.R., Mole L.A. (2007) Predictors of response of US veterans to treatment for the hepatitis C virus. *Hepatology* **46**: 37–47.
9. Enomoto N., Maekawa S. (2010) HCV genetic elements determining the early response to peginterferon and ribavirin therapy. *Intervirology* **53**: 66–9.
10. Enomoto N., Sakuma I., Asahina Y., Kurosaki M., Murakami T., Yamamoto C., Ogura Y., Izumi N., Marumo F., Sato C. (1996) Mutations in the nonstructural protein 5A gene and response to interferon in patients with chronic hepatitis C virus 1b infection. *N Engl J Med* **334**: 77–81.
11. El-Shamy A., Nagano-Fujii M., Sasase N., Imoto S., Kim S.R., Hotta H. (2008) Sequence variation in hepatitis C virus nonstructural protein 5A predicts clinical outcome of pegylated interferon/ribavirin combination therapy. *Hepatology* **48**: 38–47.
12. Akuta N., Suzuki F., Kawamura Y., Yatsuji H., Sezaki H., Suzuki Y., Hosaka T., Kobayashi M., Kobayashi M., Arase Y., Ikeda K., Miyakawa Y., Kumada H. (2007) Prediction of response to pegylated interferon and ribavirin in hepatitis C by polymorphisms in the viral core protein and very early dynamics of viremia. *Intervirology* **50**: 361–8.
13. Akuta N., Suzuki F., Sezaki H., Suzuki Y., Hosaka T., Someya T., Kobayashi M., Saitoh S., Watahiki S., Sato J., Matsuda M., Kobayashi M., Arase Y., Ikeda K., Kumada H. (2005) Association of amino acid substitution pattern in core protein of hepatitis C virus genotype 1b high viral load and non-virological response to interferon-ribavirin combination therapy. *Intervirology* **48**: 372–80.
14. Akuta N., Suzuki F., Kawamura Y., Yatsuji H., Sezaki H., Suzuki Y., Hosaka T., Kobayashi M., Kobayashi M., Arase Y., Ikeda K., Kumada H. (2007) Predictive factors of early and sustained responses to peginterferon plus ribavirin combination therapy in Japanese patients infected with hepatitis C virus genotype 1b: Amino acid substitutions in the core region and low-density lipoprotein cholesterol levels. *J Hepatol* **46**: 403–10.
15. El-Shamy A., Kim S.R., Ide Y.H., Sasase N., Imoto S., Deng L., Shoji I., Hotta H. (2011) Polymorphisms of hepatitis C virus non-structural protein 5A and core proteins and clinical outcome of pegylated-interferon/ribavirin combination therapy. *Intervirology* (in press).
16. Sanjo M., Saito T., Ishii R., Nishise Y., Haga H., Okumoto K., Ito J., Watanabe H., Saito K., Togashi H., Fukuda K., Imai Y., El-Shamy A., Deng L., Shoji I., Hotta H., Kawata S. (2010) Secondary structure of the amino-terminal region of HCV NS3 and virological response to pegylated interferon plus ribavirin therapy for chronic hepatitis C. *J Med Virol* **82**: 1364–70.
17. Okamoto H., Sugiyama Y., Okada S., Kurai K., Akahane Y., Sugai Y., Tanaka T., Sato K., Tsuda F., Miyakawa Y., Mayumi M. (1992) Typing hepatitis C virus by polymerase chain reaction with type-specific primers: application to clinical surveys and tracing infectious sources. *J Gen Virol* **73**(Pt 3): 673–9.
18. El-Shamy A., Sasayama M., Nagano-Fujii M., Sasase N., Imoto S., Kim S.R., Hotta H. (2007) Prediction of efficient virological response to pegylated interferon/ribavirin combination therapy by NS5A sequences of hepatitis C virus and anti-NS5A antibodies in pre-treatment sera. *Microbiol Immunol* **51**: 471–82.
19. Ogata S., Nagano-Fujii M., Ku Y., Yoon S., Hotta H. (2002) Comparative sequence analysis of the core protein and its

frameshift product, the F protein, of hepatitis C virus subtype 1b strains obtained from patients with and without hepatocellular carcinoma. *J Clin Microbiol* **40**: 3625–30.
20. Fukuhara T., Taketomi A., Okano S., Ikegami T., Soejima Y., Shirabe K., Maehara Y. (2010) Mutations in hepatitis C virus genotype 1b and the sensitivity of interferon-ribavirin therapy after liver transplantation. *J Hepatol* **52**: 672–680.
21. Sasase N., Kim S.R., Kudo M., Kim K.I., Taniguchi M., Imoto S., Mita K., Hayashi Y., Shoji I., El-Shamy A., Hotta H. (2010) Outcome and early viral dynamics with viral mutation in PEG-IFN/RBV therapy for chronic hepatitis in patients with high viral loads of serum HCV RNA genotype 1b. *Intervirology* **53**: 49–54.
22. Ge D., Fellay J., Thompson A.J., Simon J.S., Shianna K.V., Urban T.J., Heinzen E.L., Qiu P., Bertelsen A.H., Muir A.J., Sulkowski M., Mchutchison J.G., Goldstein D.B. (2009) Genetic variation in IL28B predicts hepatitis C treatment-induced viral clearance. *Nature* **461**: 399–401.
23. Suppiah V., Moldovan M., Ahlenstiel G., Berg T., Weltman M., Abate M.L., Bassendine M., Spengler U., Dore G.J., Powell E., Riordan S., Sheridan D., Smedile A., Fragomeli V., Muller T., Bahlo M., Stewart G.J., Booth D.R., George J. (2009) IL28B is associated with response to chronic hepatitis C interferon-alpha and ribavirin therapy. *Nat Genet* **41**: 1100–4.
24. Tanaka Y., Nishida N., Sugiyama M., Kurosaki M., Matsuura K., Sakamoto N., Nakagawa M., Korenaga M., Hino K., Hige S., Ito Y., Mita E., Tanaka E., Mochida S., Murawaki Y., Honda M., Sakai A., Hiasa Y., Nishiguchi S., Koike A., Sakaida I., Imamura M., Ito K., Yano K., Masaki N., Sugauchi F., Izumi N., Tokunaga K., Mizokami M. (2009) Genome-wide association of IL28B with response to pegylated interferon-alpha and ribavirin therapy for chronic hepatitis C. *Nat Genet* **41**: 1105–9.
25. Shirakawa H., Matsumoto A., Joshita S., Komatsu M., Tanaka N., Umemura T., Ichijo T., Yoshizawa K., Kiyosawa K., Tanaka E. (2008) Pretreatment prediction of virological response to peginterferon plus ribavirin therapy in chronic hepatitis C patients using viral and host factors. *Hepatology* **48**: 1753–60.
26. Okanoue T., Itoh Y., Hashimoto H., Yasui K., Minami M., Takehara T., Tanaka E., Onji M., Toyota J., Chayama K., Yoshioka K., Izumi N., Akuta N., Kumada H. (2009) Predictive values of amino acid sequences of the core and NS5A regions in antiviral therapy for hepatitis C: a Japanese multi-center study. *J Gastroenterol* **44**: 952–63.
27. Hayashi K., Katano Y., Ishigami M., Itoh A., Hirooka Y., Nakano I., Urano F., Yoshioka K., Toyoda H., Kumada T., Goto H. (2011) Mutations in the core and NS5A region of hepatitis C virus genotype 1b and correlation with response to pegylated-interferon-alpha 2b and ribavirin combination therapy. *J Viral Hepat* **18**: 280–86
28. Gale M. Jr., Blakely C.M., Kwieciszewski B., Tan S.L., Dossett M., Tang N.M., Korth M.J., Polyak S.J., Gretch D.R., Katze M.G. (1998) Control of PKR protein kinase by hepatitis C virus nonstructural 5A protein: molecular mechanisms of kinase regulation. *Mol Cell Biol* **18**: 5208–18.
29. Moradpour D., Evans M.J., Gosert R., Yuan Z., Blum H.E., Goff S.P., Lindenbach B.D., Rice C.M. (2004) Insertion of green fluorescent protein into nonstructural protein 5A allows direct visualization of functional hepatitis C virus replication complexes. *J Virol* **78**: 7400–9.
30. Appel N., Pietschmann T., Bartenschlager R. (2005) Mutational analysis of hepatitis C virus nonstructural protein 5A: potential role of differential phosphorylation in RNA replication and identification of a genetically flexible domain. *J Virol* **79**: 3187–94.
31. Yuan H.J., Jain M., Snow K.K., Gale M. Jr., Lee W.M. (2009) Evolution of hepatitis C virus NS5A region in breakthrough patients during pegylated interferon and ribavirin therapy. *J Viral Hepat* **17**: 208–216.
32. Bode J.G., Ludwig S., Ehrhardt C., Albrecht U., Erhardt A., Schaper F., Heinrich P.C., Haussinger D. (2003) IFN-alpha antagonistic activity of HCV core protein involves induction of suppressor of cytokine signaling-3. *Faseb J* **17**: 488–90.
33. De Lucas S., Bartolome J., Carreno V. (2005) Hepatitis C virus core protein down-regulates transcription of interferon-induced antiviral genes. *J Infect Dis* **191**: 93–99.

NS5A-IRRDR変異数

NS5A-interferon/ribavirin resistance-determining region(IRRDR)

勝二郁夫(写真)　Ahmed El-Shamy　堀田　博
Ikuo Shoji, Ahmed El-Shamy and Hak Hotta
神戸大学大学院医学研究科微生物学分野

◎遺伝子型1bのC型慢性肝炎に対するペグ(pegylated)-インターフェロン・リバビリン(PEG-IFN/RBV)治療応答性の予測にNS5A-IRRDR変異が有用であり，IRRDR>6はsustained virological response(SVR)と高い相関をもつ．IRRDR変異は独立予測因子であり，他の予測因子と組み合わせることにより，さらに精度の高い予測因子となる．他の遺伝子型2a，2b，4aのPEG-IFN/RBV併用療法においても，IRRDR変異はSVR予測に有用である．IRRDR領域の前後の配列は高度に保存されているが，IRRDR領域は各遺伝子型で多様性に富んでおり，PEG-IFN/RBV療法感受性を規定する分子機構を考えるうえで興味深い．

Key word：C型肝炎ウイルス(HCV)，PEG-IFN/RBV，NS5A，IRRDR

C型慢性肝炎の標準的治療法であるペグインターフェロン＋リバビリン(PEG-IFN/RBV)併用療法の予後に影響する因子は，①ウイルス側因子，②宿主因子，③治療因子，の3つに大別される．ウイルス側因子としては遺伝子型，ウイルス量，ゲノムの多様性が重要である．著者らはC型肝炎ウイルス(HCV)のNS5Aの遺伝子多様性に注目し，HCV-1bのPEG-IFN/RBV療法予後予測因子として，IFN/RBV resistance-determining region(IRRDR)の有用性を報告してきた[1-5]．

HCV NS5A蛋白質とIRRDR変異数

HCVのNS5A蛋白質はリン酸化蛋白質で低リン酸化型(p56)と超リン酸化型(p58)が存在し，HCVのゲノム複製に必須の蛋白質である[6]．蛋白質リン酸化酵素casein kinase I[7]やcasein kinase II[8]がNS5Aの超リン酸化に関与するという報告があるが，それ以外にも多数のリン酸化酵素の関与が報告されており[9]，制御機構は不明な点が多い．NS5A蛋白質は3つのドメイン構造を有し，domain I(HCV蛋白質全体ではaa1973-2185；NS5A内ではaa27-213)，domain II(aa2222-2314；aa250-342)，domain III(aa2328-2419；aa356-447)からなる(図1)．domain IはRNA結合能を有し，domain IIにはinterferon sensitivity determining region(ISDR)[10]が含まれている．domain IIIはNS5Aの粒子形成に重要とする知見が報告されている[11,12]．

著者らは，domain IIIのなかでも従来からV3領域[13]とよばれていた部分を含む46アミノ酸からなるIRRDR(aa2334-2379)領域の配列がHCV-1b症例におけるPEG-IFN/RBV療法応答性と高い相関を示すことを見出した[1]．IRRDR変異数(「サイドメモ」参照)はISDR領域の解析と同様に，コンセンサス配列であるHCV-J株のNS5Aと同部位を比較し，IRRDRに6個以上のアミノ酸変異がある(IRRDR≧6)場合にPEG-IFN/RBV療法で早期にウイルスが消失し，sustained virological response(SVR；治療終了後24終後でHCV-RNAが陰性，著効)となり，5個以下の変異である

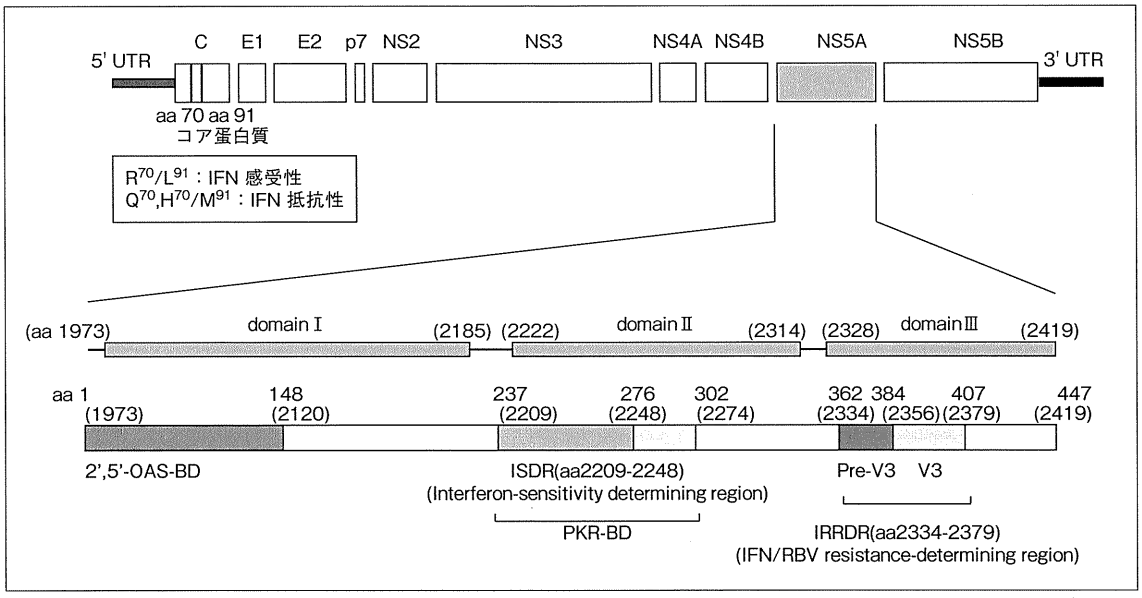

図 1　HCV genotype 1bのPEG-IFN/RBV療法の治療効果予測に関するウイルス因子

core aa70，aa91 アミノ酸置換．
NS5A-ISDR：interferon sensitivity determining region.
NS5A-IRRDR：interferon/ribavirin resistance-determining region.
2′, 5′-OAS-BD：2′, 5′-oligoadenylate synthetase-binding domain.
PKR-BD：PKR-binding domain.
aa：アミノ酸．アミノ酸番号はNS5A 蛋白質での番号．（ ）内はHCV 蛋白質でのアミノ酸番号．

(IRRDR≦5)場合に治療抵抗性である傾向が強いことを報告した[2]．

NS5A-IRRDR変異数と他の予測因子

前項で詳述されているように，IRRDR 以外にも，IFN 療法応答性予測因子としてISDR[10]，Core アミノ酸置換[14]が報告されている．そこで，各IFN 療法応答性予測因子を組み合わせることでより精度の高い予測因子となるか検討するために，HCV-1b，PEG-IFN/RBV 療法施行 68 症例の治療前血清を解析し，IRRDR とその他の予測因子の治療成績との関係を解析した[4]．IRRDR≧

サイドメモ

NS5A-IRRDR配列の解析方法

QIAmp viral RNA kit(QIAGEN，Tokyo)を用いて，治療前血清 140 μL から HCV-RNA を抽出し，Super-Script One-step RT-PCR for long templates (Invitrogen，Tokyo)で逆転写反応を行う．1st RT-PCR は NS5A-F1(5′-TACTCCCTGCCATCCCTCTCCTG-3′；sense primer，nucleotides [nt] 5974-5997)と NS5A-F2(5′-CTCCTTGAGCACGTCCCGGT-3′；antisense primer，nt7796-7777)でNS5A 領域を増幅する．2nd PCR は Platinum Taq DNA polymerase(Invitrogen)で内部プライマー，NS5A-F3 (5′-TCTCCAGCCTTACCATCACYCA-3′；sense primer，nt6172-6193；Y=C or T)と NS5A-F4 (5′-CGGTARTGRTCGTCCAGGAC-3′；antisense primer，nt7780-7761；R=A or G)を使用．逆転写反応は 45℃，30 min，94℃，2 min．ついで 1st PCR と 2nd PCR は(94℃，30 sec；55℃，30 sec；68℃，90 sec)×35 サイクル．2nd PCR 産物を QIA quick PCR amplification kit(QIAGEN)で精製し，ダイレクトシークエンス法で塩基配列決定し，HCV-J 株の NS5A と配列を比較する[1]．

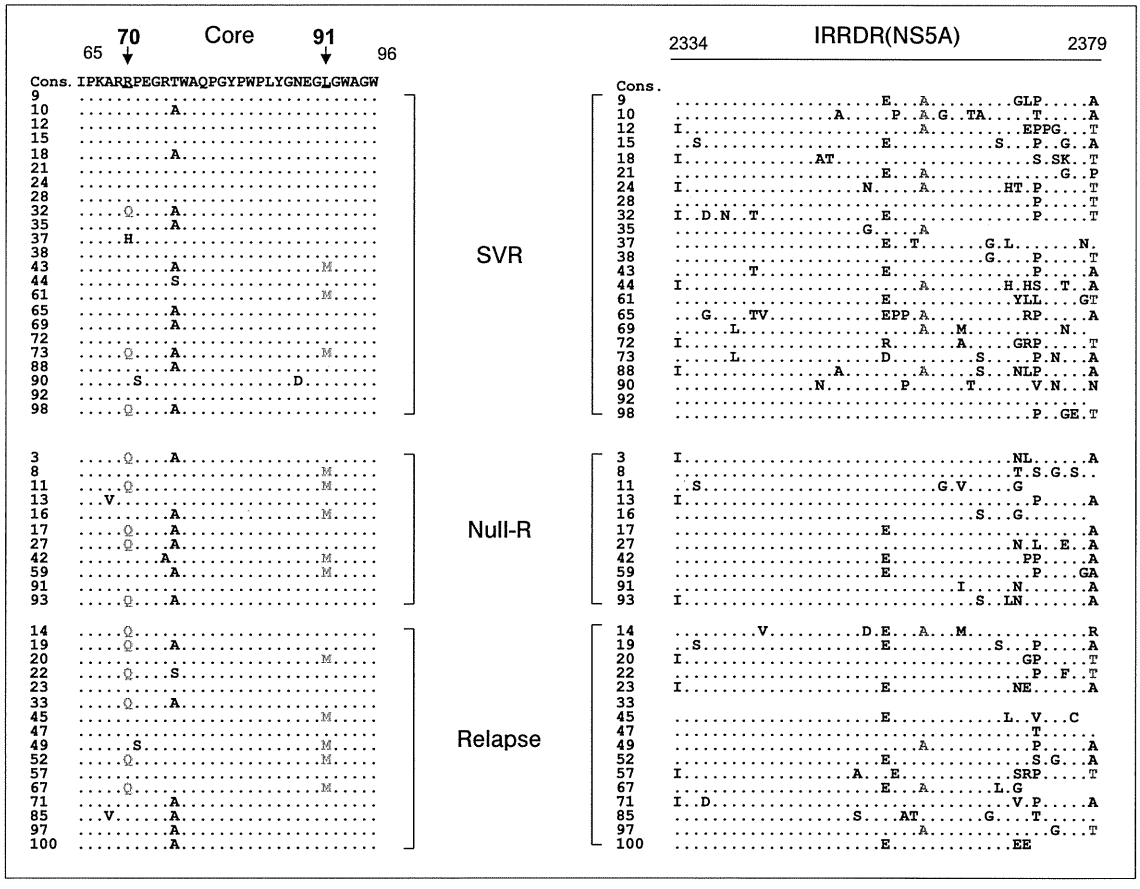

図 2　HCVコア蛋白質およびNS5Aのアミノ酸配列多様性とSVRとの相関

6である24例中18例(75%)でSVRになったが，IRRDR≦5の44例中では11例(25%)しかSVRにならなかった．IRRDR≧6はSVRと有意な相関を示した($p<0.0001$)．一方，ISDR≧2はrelapse(治療終了時はHCV-RNAが陰性化しているが，治療後に再陽性化)と有意な相関を示した($p<0.05$)．また，Coreアミノ酸置換70Qがnull virological response(治療期間中HCV-RNAが持続陽性，無効)と有意な相関を示した($p<0.05$)．IRRDR≧6とCore R^{70}/L^{91}はHCV RNA早期陰性化と相関した．多変量解析を行ったところ，IRRDR≧6とCore R^{70}/L^{91}は独立予測因子と考えられ(図2)，両因子を組み合わせることにより，より有用な治療効果予測になる可能性が示された[4]．

HCV-2a，2bにおけるIRRDR変異数

つぎに，遺伝子型2a，2b，4aなどの他の遺伝子型において，NS5A配列の多様性とIFN/RBV療法応答性との関連について解析を行った．HCV-4aはエジプトで多く[15]，IFN/RBV療法に抵抗性であることが知られている．

PEG-IFN-α-2b/RBV併用療法を24週間施行した後，24週の経過を観察できた88症例について解析した．遺伝子型2は1bに比べると治療成績は良好で，全体で83%のSVRが得られた．HCV-2aでは89%，HCV-2bでは77%のSVR率で2aのほうが2bより若干成績が良好であった．遺伝子型2aのNS5A配列の多様性と治療効果の相関を調べるためにrapid virological response(RVR；治療4週目までにHCV-RNAが陰性化)症例とnon-RVR症例を比較した．この結果，RVRとnon-RVRではNS5AのC末端側の2カ所の領域

でアミノ酸変異に有意な差があった．ひとつはISDRとそのC末端側を含む領域(aa2232-2262)のISDR/＋C[2a]，もうひとつはIRRDRに相当する領域(aa2332-2387)のIRRDR[2a]であった．RVR症例ではIRRDR[2a]に有意に変異が多く，IRRDR[2a]≧4でSVR症例が多かった．また，IRRDR≧4で治療前のウイルス価が有意に低く，治療後にCore抗原が速やかに減少していた．

遺伝子型2bに関してはIRRDRのN末端側にRVRとnon-RVRで変異数に有意な差がある領域(aa2332-2387)がみつかった．これをIRRDR/N[2b]と名づけ配列を比較した．RVR症例ではIRRDR/N[2b]に多くのアミノ酸変異が認められた．

以上の結果から，遺伝子型2a，2bでもNS5Aの多様性は治療応答性と相関があり，IRRDR[2a]≧4はSVR，RVRと有意に相関した．遺伝子型2bに関してはIRRDR/N[2b]≧2がRVRと有意な相関を示した．RVRおよびSVRと相関する因子について単変量解析，多変量解析を行ったところ，IRRDR[2a]≧4のみが有意な相関を示し，予測因子として有用性が期待できた(El-Shamyら，投稿中)．

HCV-4aにおけるIRRDR変異数

最後に遺伝子型4aにおいて，SVRとNon-SVRでIRRDR[4a](aa2331-2383)の変異数に有意な差を認めた．遺伝子型4aは症例数も少なくさらに検討を重ねる必要があるが，IRRDR[4a]≧4ではSVRが80%，IRRDR[4a]≦3ではnon-SVRが76%であり，遺伝子型4aにおいてもIRRDR変異が治療応答性と密接に関与していることが示唆された．

HCVすべての遺伝子型においてIRRDR領域の前後の配列は高度に保存されているが，IRRDR領域は多様性に富んでおり，PEG-IFN/RBV療法感受性を規定する分子機構を考えるうえで興味深い．

文献

1) El-Shamy, A. et al.: Prediction of efficient virological response to pegylated interferon/ribavirin combination therapy by NS5A sequences of hepatitis C virus and anti-NS5A antibodies in pretreatment sera. *Microbiol. Immunol.*, **51**: 471-482, 2007.
2) El-Shamy, A. et al.: Sequence variation in hepatitis C virus nonstructural protein 5 A predicts clinical outcome of pegylated interferon/ribavirin combination therapy. *Hepatology*, **48**: 38-47, 2008.
3) Sasase, N. et al.: Outcome and early viral dynamics with viral mutation in PEG-IFN/RBV therapy for chronic hepatitis in patients with high viral loads of serum HCV RNA genotype 1b. *Intervirology*, **53**: 49-54, 2010.
4) El-Shamy, A. et al.: Polymorphisms of hepatitis C virus non-structural protein 5 A and core protein and clinical outcome of pegylated-interferon/ribavirin combination therapy. *Intervirology*, **55**: 1-11, 2012.
5) El-Shamy, A. et al.: Sequence heterogeneity of NS5A and core proteins of hepatitis C virus and virological responses to pegylated-interferon/ribavirin combination therapy. *Microbiol. Immunol.*, **55**: 418-426, 2011.
6) Moradpour, D. et al.: Replication of hepatitis C virus. *Nat. Rev. Microbiol.*, **5**: 453-463, 2007.
7) Quintavalle, M. et al.: The alpha isoform of protein kinase CKI is responsible for hepatitis C virus NS5A hyperphosphorylation. *J. Virol.*, **80**: 11305-11312, 2006.
8) Kim, S. O. et al.: Ischemia induced activation of heat shock protein 27 kinases and casein kinase 2 in the preconditioned rabbit heart. *Biochem. Cell Biol.*, **77**: 559-567, 1999.
9) Chen, Y. C. et al.: Polo-like kinase 1 is involved in hepatitis C virus replication by hyperphosphorylating NS5A. *J. Virol.*, **84**: 7983-7993, 2010.
10) Enomoto, N. et al.: Mutations in the nonstructural protein 5 A gene and response to interferon in patients with chronic hepatitis C virus 1b infection. *N. Engl. J. Med.*, **334**: 77-81, 1996.
11) Tellinghuisen, T. L. et al.: Regulation of hepatitis C virion production via phosphorylation of the NS5A protein. *PLoS Pathog.*, **4**: e1000032, 2008.
12) Masaki, T. et al.: Interaction of hepatitis C virus nonstructural protein 5 A with core protein is critical for the production of infectious virus particles. *J. Virol.*, **82**: 7964-7976, 2008.
13) Inchauspe, G.: DNA vaccine strategies for hepatitis C. *J. Hepatol.*, **30**: 339-346, 1999.
14) Akuta, N. et al.: Predictive factors of early and sustained responses to peginterferon plus ribavirin combination therapy in Japanese patients infected with hepatitis C virus genotype 1b: amino acid substitutions in the core region and low-density lipoprotein cholesterol levels. *J. Hepatol.*, **46**: 403-410, 2007.
15) Sievert, W. et al.: A systematic review of hepatitis C virus epidemiology in Asia, Australia and Egypt. *Liver Int.*, **31** (Suppl. 2): 61-80, 2011.

C型肝炎ウイルスNS5A領域のISDR・IRRDRとインターフェロン治療効果予測

勝二郁夫* Ahmed El-Shamy* 堀田博*

索引用語：HCV, IFN, PEG-IFN/RBV, NS5A, ISDR, IRRDR

1 はじめに

C型慢性肝炎の標準的治療法であるPEG-IFN/RBV併用療法の予後に影響する因子は，1)ウイルス側因子，2)宿主因子，3)治療因子の3つに大別される．ウイルス側因子としてはウイルス量，genotype，ウイルスゲノムの多様性が重要である．宿主因子としては高年齢女性，肝線維化進展例，血小板数，赤血球数に加え，*IL28B* SNPs[1]が重要とされている．治療因子は治療法，投与期間，薬剤指示遵守度があげられる．

HCV genotype 1bの慢性肝炎のインターフェロン(IFN)治療成績と相関を示すウイルス側因子として，NS5A領域のInterferon sensitivity determining region (ISDR)[2,3]，Interferon/ribavirin resistance-determining region (IRRDR)[4,5]とCoreアミノ酸(aa 70・91)置換[6,7]が報告されている．

本稿ではNS5A領域のISDR, IRRDRについて詳述したい．

HCVのNS5A蛋白質はリン酸化蛋白質で低リン酸化型(p56)と超リン酸化型(p58)が存在し，HCVのゲノム複製に必須の蛋白質である[8]．蛋白質リン酸化酵素casein kinase I[9]やcasein kinase II[10]がNS5Aの超リン酸化に関与するという報告があるが，それ以外にも多数のリン酸化酵素の関与が報告されており[11]，制御機構は不明な点が多い．NS5A蛋白質は三つのドメイン構造を有し，domain I (HCV蛋白質全体ではaa 1973-2185; NS5A内ではaa 27-213)，domain II (aa 2222-2314; aa 250-342)，domain III (aa 2328-2419；aa 356-447)からなる(図1)．domain IはRNA結合能を有し，domain IIのaa 2209-2248にはISDR[3]が存在する．domain IIIはNS5Aの粒子形成に重要であることが報告されている[12,13]．domain IIIの従来V3領域[14]と呼ばれていた部分を含む46アミノ酸(aa 2334-2379)からなるIRRDR領域の配列の多様性がHCV-1b症例におけるPEG-IFN/RBV療法応答性と高い相関を示すことをわれわれは報告した[4]．

Ikuo SHOJI et al: Hepatitis C virus NS5A-ISDR and -IRRDR as predictive markers for interferon therapy
*神戸大学大学院医学研究科微生物学分野［〒650-0017 兵庫県神戸市中央区楠町7-5-1］

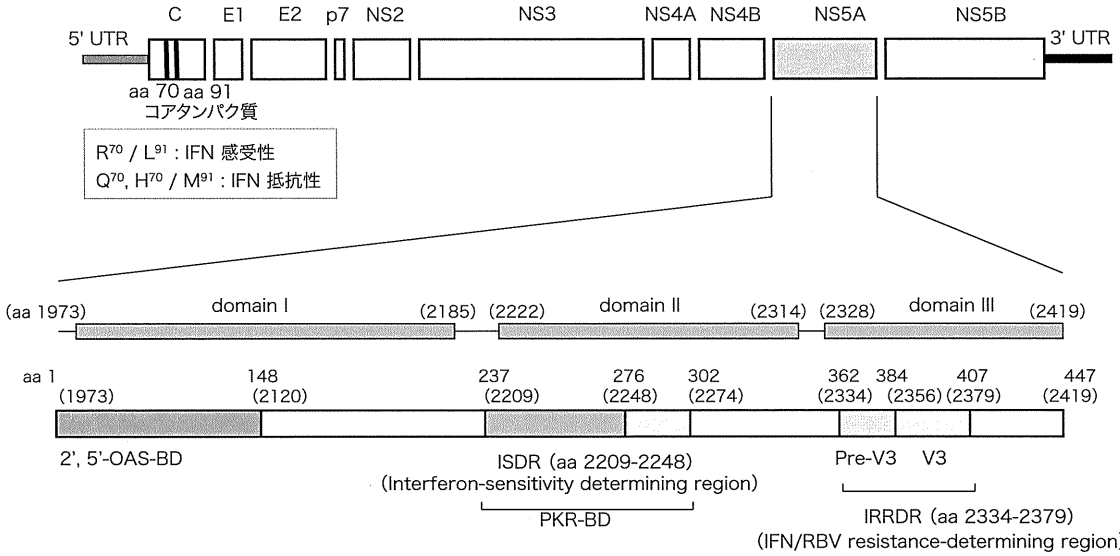

図1　HCV genotype 1bのPEG-IFN/RBV療法の治療効果予測に関するウイルス因子
core aa70, aa91アミノ酸置換，NS5A-ISDR: Interferon sensitivity determining region, NS5A-IRRDR: Interferon/ribavirin resistance-determining region. 2', 5' -OAS-BD: 2', 5' -oligoadenylate synthetase-binding domain. PKR-BD: PKR-binding domain.
aa：アミノ酸．アミノ酸番号はNS5A蛋白質での番号．括弧内はHCV蛋白質でのアミノ酸番号．

表1　C型肝炎ウイルスに対するIFN療法のウイルス学的治療効果判定

判定方法	治療効果判定
治療4週目までにHCV RNAが陰性化	rapid virological response (RVR)
治療12週目までにHCV RNAが陰性化	complete early virological response (cEVR)
治療12週目までにHCV RNAが2 log以上減少するが，陰性化しない	partial early virological response (pEVR)
治療13～24週目の間にHCV RNAが陰性化する	late virological response (LVR)
治療期間中HCV RNAが持続陽性（無効）	null virological respnse (NVR)
治療終了時はHCV RNAが陰性化しているが，治療後に再陽性化(再燃)	relapse
治療終了24週後でHCV RNAが陰性（著効）	sustained virological response (SVR)

2　IFN単独療法とISDR

榎本信幸博士(山梨大学医学部第一内科教授)らはHCV NS5Aの多様性とIFN感受性の相関を世界に先駆けて報告した[2,3]．HCV genotype 1bのC型慢性肝炎に対する6カ月間のIFN単独療法において，著効例と無効例の全塩基配列を比較検討し，インターフェロン感受性を規定するウイルス側因子としてISDR領域(aa 2209-2248)を報告した．HCV-1bの標準株HCV-J株のISDR領域と比較し，変異のない野生型(wild type)，1～3個の変異がある中間型(intermediate type)，4個以上変異のある変異型(mutant type)に分類すると変異型で特にIFN感受性が増し，Sustained virological response (SVR)率(表1)が上昇することを報告した[3]．

また，PEG-IFN/RBV併用療法においても

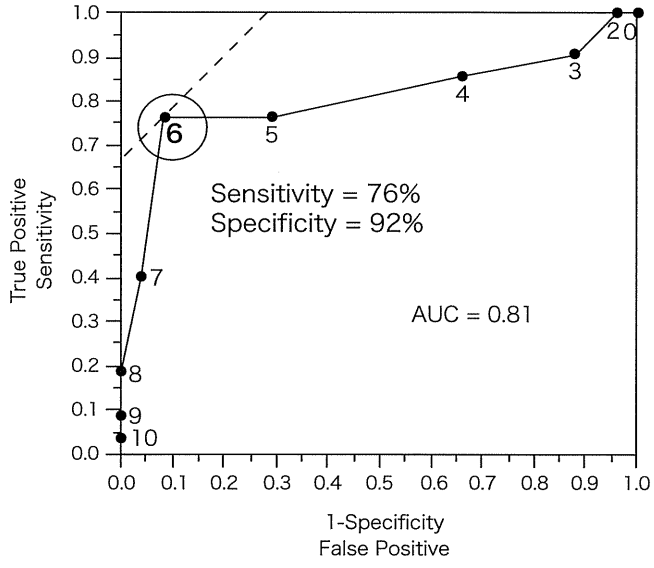

図2　SVR予測のための最適IRRDR変異数
Receiver Operating Characteristic Curve（ROC）解析によりIRRDR≥6とIRRDR≤5で分けると最適となる．

ISDRは治療後4週目までのHCV RNAの陰性化（Rapid virological response; RVR）とよく相関することが報告されている[15]．

3　PEG-IFN/RBV併用療法とIRRDR

IFN単独24週投与のSVR率はHCV-1b・高ウイルス量の難治例では10％程度，全体でも30～40％と不十分な結果であった．しかし，IFN/RBV併用療法24週投与，そしてPEG-IFN/RBV療法48週投与の導入により，HCV-1bの難治例においてもSVR率が50％近くにまで上昇した．ところが，依然として治療抵抗性を示す症例が半数近くあることから，PEG-IFN/RBV療法の抵抗性に関与するウイルス側因子の探索が進められた．

われわれは神戸朝日病院の金守良博士との共同研究で，HCV-1bのPEG-IFN/RBV併用療法における，治療前のウイルスゲノムと治療成績との関係を解析した．Sliding window analysisにより，domain III（aa 2334-2379）の46アミノ酸からなるIRRDR領域の配列が，PEG-IFN/RBV療法の応答性と高い相関を示すことをみいだした[4,5]．そして，予後予測因子としてIRRDR変異数が臨床上有用であることを提唱してきた[4,5,16～18]．IRRDR変異数の解析方法は，ISDR領域の解析と同様に行われる[4]．コンセンサス配列のHCV-J株のNS5A-IRRDR領域と治療前のNS5A-IRRDR領域のアミノ酸配列を比較し，IRRDRに6個以上のアミノ酸変異がある（IRRDR≥6）場合にはPEG-IFN/RBV療法で早期にウイルスが消失しSVRとなり，5個以下の変異である（IRRDR≤5）場合に治療抵抗性となる傾向が強いことを報告した[5]．ここで，治療効果予測に適したIRRDR変異数のカットオフ値はReceiver operating characteristic curve（ROC）解析によって求めている（図2）．

河田純男博士（前山形大学医学部消化器内科教授．現，兵庫県立西宮病院長）との共同研究[18]で，57例のHCV-1b症例の解析から，

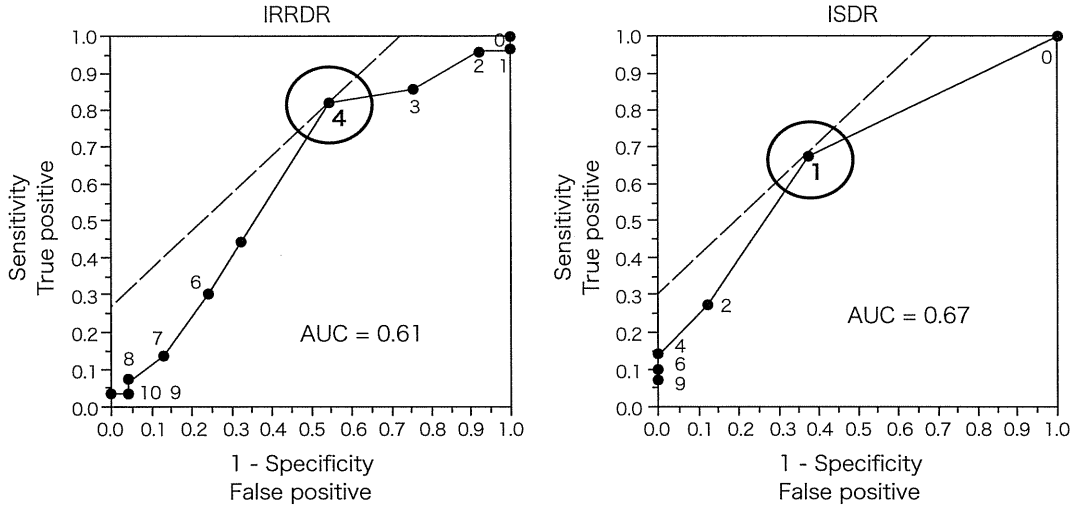

図3　SVR予測のためのIRRDRおよびISDRの最適変異数
山形県のサンプルのROC解析の結果ではIRRDR≥4とIRRDR≤3で分けると最適となった.

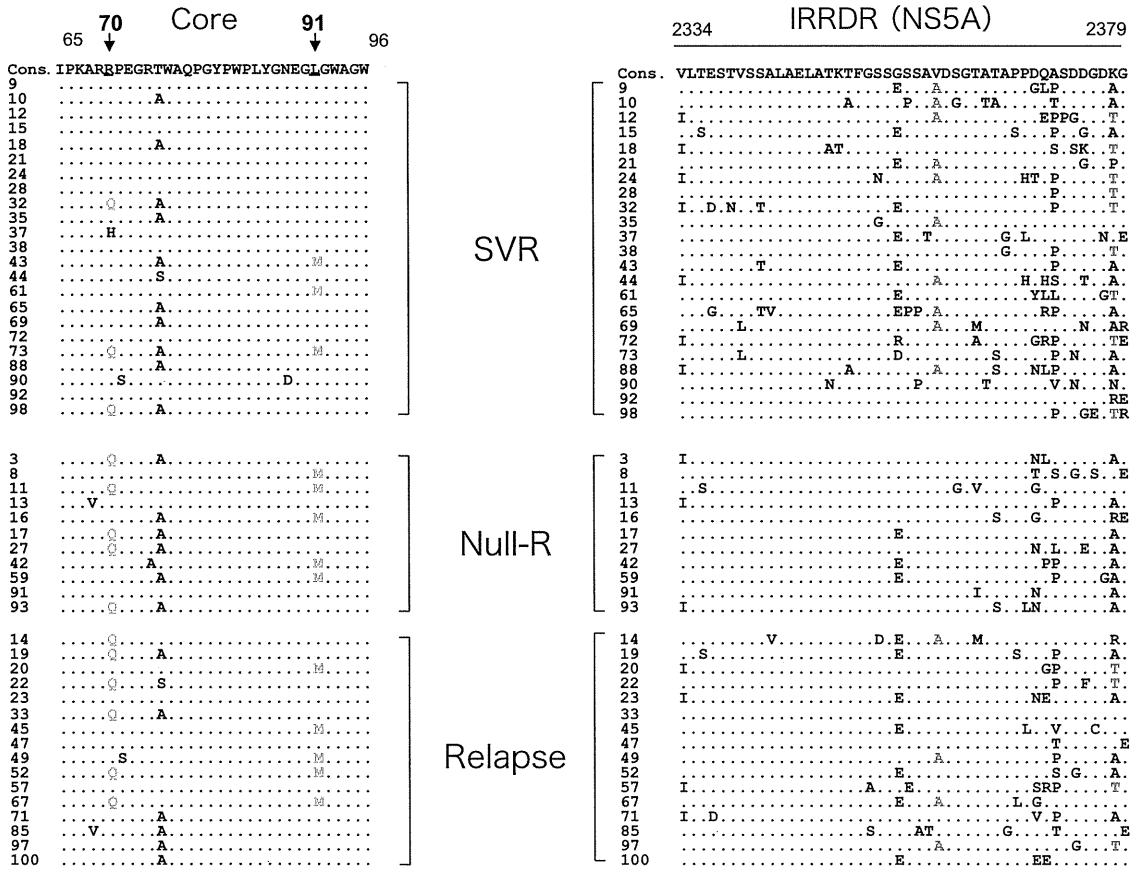

図4　HCV-1b コアタンパク質およびNS5Aのアミノ酸配列多様性とSVRとの相関

IRRDR≥4でSVR率70%，IRRDR≤3でSVR率が24%であり，IRRDRのカットオフ値に若干の変動はあったものの(図3)，別の患者群でもIRRDR変異数が多いとSVR率が高く，IRRDR変異数が少ないとSVR率が低いという結果が得られ，IRRDR変異数の有用性が示唆された．

4 NS5A-IRRDRと他の予測因子

上述したように，IRRDR以外にも，IFN療法応答性予測因子としてISDR[3]，Coreアミノ酸置換[7]が報告されている．そこで，HCV-1b, PEG-IFN/RBV療法施行68症例の治療前血清を解析し，IRRDRとその他の予測因子の治療成績との関係を解析した[17]．IRRDR≥6である24例中18例(75%)でSVRになったが，IRRDR≤5の44例中では11例(25%)しかSVRにならなかった．IRRDR≥6はSVRと有意な相関を示した($p<0.0001$)．一方，ISDR≥2はrelapse(治療終了時はHCV RNAが陰性化しているが，治療後に再陽性化)と有意な相関を示した($p<0.05$)．また，Coreアミノ酸置換Q^{70}がnull virological response(NVR:治療期間中HCV RNAが持続陽性，無効)と有意な相関を示した($p<0.05$)．IRRDR≥6とCore R^{70}/L^{91}はHCV RNA早期陰性化と相関した．多変量解析を行ったところ，IRRDR≥6とCore R^{70}/L^{91}は独立予測因子と考えられ(図4)，両因子を組み合わせることにより，より有用な治療効果予測になる可能性が示された．

5 HCV-2a, 2bにおけるIRRDR

次に，HCV-2a, -2bのgenotypeにおいてNS5A配列の多様性とPEG-IFN/RBV療法応答性との関連について解析を進めた．PEG-IFNα-2b/RBV併用療法24週間施行した後，24週経過観察できた88症例について解析した．HCV-2a/-2bはHCV-1bに比べると治療成績は良好で全体で83%のSVRが得られた．HCV-2aでは89%，HCV-2bでは77%のSVR率で2aの方が2bより若干成績が良好であった．HCV-2aのNS5A配列の多様性と治療効果の相関を調べるためにRapid virological response (RVR: 治療4週目までにHCV RNAが陰性化)症例とnon-RVR症例を比較した(表1)．この結果，RVRとnon-RVRではNS5AのC末端側の2カ所の領域でアミノ酸変異に有意な差があった．一つはISDRとそのC末端側を含む領域(aa 2232-2262)のISDR/+C[2a]，もう一つはIRRDRに相当する領域(aa 2332-2387)のIRRDR[2a]であった．RVR症例では，IRRDR[2a]に有意に変異が多く，IRRDR[2a]≥4でSVR症例が多かった．また，IRRDR≥4で治療前のウイルス価が有意に低く，治療後にCore抗原量が速やかに減少していた．

HCV-2bに関してはIRRDRのN末端側にRVRとnon-RVRで変異数に有意な差がある領域(aa 2332-2387)がみつかった．これをIRRDR/N[2b]と名付け配列を比較したところ，RVR症例ではIRRDR/N[2a]に多くのアミノ酸変異が認められた．

以上の結果から，HCV-2a, -2bでもNS5Aの多様性は治療応答性と相関があり，IRRDR[2a]≥4はSVR, RVRと有意に相関した．HCV-2bに関してはIRRDR/N[2b]がRVRと有意な相関を示した．RVRおよびSVRと相関する因子について単変量解析，多変量解析を行ったところ，IRRDR[2a]≥4のみが有意な相関を示し，予測因子として有用性が期待できた(El-Shamy et al. 投稿中)．

6 HCV-4aにおけるIRRDR

さらにHCV-4aにおけるIRRDRの有用性を解析した．HCV-4aはエジプトで多く，IFN/RBV療法に抵抗性であることが知られている．HCV-4aにおいて，SVRとNon-SVRでIRRDR[4a]（aa 2331-2383）の変異数に有意な差を認めた．HCV-4は症例数も少なくさらに検討を重ねる必要があるが，IRRDR[4a]≥4ではSVRが80％，IRRDR[4a]≤3ではnon-SVRが76％であり，HCV-4aにおいてもIRRDR変異が治療応答性と密接に関与していることが示唆された（El-Shamy et al., 投稿準備中）．

HCVすべてのgenotypeにおいてIRRDR領域の前後の配列は高度に保存されているが，IRRDR領域は多様性に富んでおり，PEG-IFN/RBV療法感受性を規定する分子機構を考えるうえで興味深い．

文　献

1) Tanaka Y, Nishida N, Sugiyama M et al : Genome-wide association of IL28B with response to pegylated interferon-alpha and ribavirin therapy for chronic hepatitis C. Nat Genet 41 : 1105–1109, 2009
2) Enomoto N, Sakuma I, Asahina Y et al : Comparison of full-length sequences of interferon-sensitive and resistant hepatitis C virus 1b. Sensitivity to interferon is conferred by amino acid substitutions in the NS5A region. J Clin Invest 96 : 224–230, 1995
3) Enomoto N, Sakuma I, Asahina Y et al : Mutations in the nonstructural protein 5A gene and response to interferon in patients with chronic hepatitis C virus 1b infection. N Engl J Med 334 : 77–81, 1996
4) El-Shamy A, Sasayama M, Nagano-Fujii M et al : Prediction of efficient virological response to pegylated interferon/ribavirin combination therapy by NS5A sequences of hepatitis C virus and anti-NS5A antibodies in pre-treatment sera. Microbiol Immunol 51 : 471–482, 2007
5) El-Shamy A, Nagano-Fujii M, Sasase N et al : Sequence variation in hepatitis C virus nonstructural protein 5A predicts clinical outcome of pegylated interferon/ribavirin combination therapy. Hepatology 48 : 38–47, 2008
6) Akuta N, Suzuki F, Sezaki H et al : Association of amino acid substitution pattern in core protein of hepatitis C virus genotype 1b high viral load and non-virological response to interferon-ribavirin combination therapy. Intervirology 48 : 372–380, 2005
7) Akuta N, Suzuki F, Kawamura Y et al : Predictive factors of early and sustained responses to peginterferon plus ribavirin combination therapy in Japanese patients infected with hepatitis C virus genotype 1b: amino acid substitutions in the core region and low-density lipoprotein cholesterol levels. J Hepatol 46 : 403–410, 2007
8) Moradpour D, Penin F, Rice CM : Replication of hepatitis C virus. Nat Rev Microbiol 5 : 453–463, 2007
9) Quintavalle M, Sambucini S, Di Pietro C et al : The alpha isoform of protein kinase CKI is responsible for hepatitis C virus NS5A hyperphosphorylation. J Virol 80 : 11305–11312, 2006
10) Kim SO, Baines CP, Critz SD et al : Ischemia induced activation of heat shock protein 27 kinases and casein kinase 2 in the preconditioned rabbit heart. Biochem Cell Biol 77 : 559–567, 1999
11) Chen YC, Su WC, Huang JY et al : Polo-like kinase 1 is involved in hepatitis C virus replication by hyperphosphorylating NS5A. J Virol 84 : 7983–7993, 2010
12) Tellinghuisen TL, Foss KL, Treadaway J : Regulation of hepatitis C virion production via phosphorylation of the NS5A protein. PLoS Pathog 4 : e1000032, 2008
13) Masaki T, Suzuki R, Murakami K et al : Interaction of hepatitis C virus nonstructural protein 5A with core protein is critical for the production of infectious virus particles. J Virol 82 : 7964–7976, 2008
14) Inchauspé G : DNA vaccine strategies for hepatitis C. J Hepatol 30 : 339–346, 1999
15) Enomoto N, Maekawa S : HCV genetic elements determining the early response to peginterferon and ribavirin therapy. Intervirology 53 : 66–69, 2010

16) Sasase N, Kim SR, Kudo M et al : Outcome and early viral dynamics with viral mutation in PEG-IFN/RBV therapy for chronic hepatitis in patients with high viral loads of serum HCV RNA genotype 1b. Intervirology 53 : 49–54, 2010
17) El-Shamy A, Kim SR, Ide YH et al : Polymorphisms of hepatitis C virus non-Structural protein 5A and core protein and clinical outcome of pegylated-interferon/ribavirin combination therapy. Intervirology 2011
18) El-Shamy A, Shoji I, Saito T et al : Sequence heterogeneity of NS5A and core proteins of hepatitis C virus and virological responses to pegylated-interferon/ribavirin combination therapy. Microbiol Immunol 55 : 418–426, 2011

*　　*　　*

THE JOURNAL OF BIOLOGICAL CHEMISTRY VOL. 286, NO. 43, pp. 37264–37273, October 28, 2011

Role of the Endoplasmic Reticulum-associated Degradation (ERAD) Pathway in Degradation of Hepatitis C Virus Envelope Proteins and Production of Virus Particles*[S]

Received for publication, May 7, 2011, and in revised form, August 18, 2011 Published, JBC Papers in Press, August 30, 2011, DOI 10.1074/jbc.M111.259085

Mohsan Saeed[§], Ryosuke Suzuki[‡], Noriyuki Watanabe[‡], Takahiro Masaki[‡], Mitsunori Tomonaga[‡], Amir Muhammad[¶], Takanobu Kato[‡], Yoshiharu Matsuura[‖], Haruo Watanabe[§], Takaji Wakita[‡], and Tetsuro Suzuki[‡ ‡‡1]**

*From the [‡]Department of Virology II, National Institute of Infectious Diseases, Tokyo 162-8640, Japan, the [§]Department of Infection and Pathology, Graduate School of Medicine, the University of Tokyo, Tokyo 113-0033, Japan, the [¶]Department of Pathology, Khyber Girls Medical College, Peshawar 25000, Pakistan, the [‖]Research Institute of Microbial Diseases, Osaka University, Osaka 565-0871, Japan, the **National Institute of Infectious Diseases, Tokyo 162-8640, Japan, and the [‡‡]Department of Infectious Diseases, Hamamatsu University School of Medicine, Hamamatsu 431-3192, Japan*

Background: HCV causes ER stress in the infected cells.
Results: HCV-induced ER stress leads to increased expression of certain proteins that in turn enhance the degradation of HCV glycoproteins and decrease production of virus particles.
Conclusion: HCV infection activates the ERAD pathway, leading to modulation of virus production.
Significance: ERAD plays a crucial role in the viral life cycle.

Viral infections frequently cause endoplasmic reticulum (ER) stress in host cells leading to stimulation of the ER-associated degradation (ERAD) pathway, which subsequently targets unassembled glycoproteins for ubiquitylation and proteasomal degradation. However, the role of the ERAD pathway in the viral life cycle is poorly defined. In this paper, we demonstrate that hepatitis C virus (HCV) infection activates the ERAD pathway, which in turn controls the fate of viral glycoproteins and modulates virus production. ERAD proteins, such as EDEM1 and EDEM3, were found to increase ubiquitylation of HCV envelope proteins via direct physical interaction. Knocking down of EDEM1 and EDEM3 increased the half-life of HCV E2, as well as virus production, whereas exogenous expression of these proteins reduced the production of infectious virus particles. Further investigation revealed that only EDEM1 and EDEM3 bind with SEL1L, an ER membrane adaptor protein involved in translocation of ERAD substrates from the ER to the cytoplasm. When HCV-infected cells were treated with kifunensine, a potent inhibitor of the ERAD pathway, the half-life of HCV E2 increased and so did virus production. Kifunensine inhibited the binding of EDEM1 and EDEM3 with SEL1L, thus blocking the ubiquitylation of HCV E2 protein. Chemical inhibition of the ERAD pathway neither affected production of the Japanese encephalitis virus (JEV) nor stability of the JEV envelope protein. A co-immunoprecipitation assay showed that EDEM orthologs do not bind with JEV envelope protein. These findings highlight the crucial role of the ERAD pathway in the life cycle of specific viruses.

Quality control of proteins, such as the elimination of misfolded proteins, is largely connected with the endoplasmic reticulum (ER),[2] which is an organelle responsible for the folding and distribution of secretory proteins to their sites of action. This pathway is termed ER-associated degradation (ERAD) and is triggered by ER stress. It results in retrotranslocation of misfolded proteins into the cytosol, followed by polyubiquitylation and proteasomal degradation (1). Several viral infections have been reported to trigger the ERAD pathway (2–4); however, the role of this pathway in the life cycle of viruses remains poorly defined.

Initiation of the ERAD pathway occurs from the oligomerization and autophosphorylation of IRE1, an ER stress sensor. The activated IRE1 removes an intron from X-box-binding protein 1 (XBP1) mRNA, which then encodes a potent transcription factor for activation of genes, for example, ER degradation-enhancing α-mannosidase-like protein (EDEM). EDEM1 (5), along with its two homologs EDEM2 (6) and EDEM3 (7), as well as ER mannosidase I (ER ManI), belong to the glycoside hydrolase 47 family. EDEMs are thought to function as lectins that deliver misfolded glycoproteins to the ERAD pathway. However, the precise mechanism by which they assist in glycoprotein quality control remains unclear.

Hepatitis C virus (HCV) infection is a major cause of chronic liver disease. The RNA genome of HCV, a member of the Fla-

* This work was supported by grants-in-aid from the Ministry of Health, Labor and Welfare, and from the Ministry of Education, Culture, Sports, Science, and Technology, Japan.
[S] The on-line version of this article (available at http://www.jbc.org) contains supplemental Figs. S1–S7.
[1] To whom correspondence should be addressed: Dept. of Infectious Diseases, Hamamatsu University School of Medicine, Hamamatsu 431-3192, Japan. Tel.: 81-53-435-2336; Fax: 81-53-435-2338; E-mail: tesuzuki@hama-med.ac.jp.

[2] The abbreviations used are: ER, endoplasmic reticulum; CHX, cycloheximide; EDEM, ER degradation-enhancing α-mannosidase-like protein; ERAD, ER-associated degradation; HCV, hepatitis C virus; JEV, Japanese encephalitis virus; KIF, kifunensine; ManI, mannosidase I; m.o.i., multiplicity of infection; TM, tunicamycin; XBP1, X-box-binding protein 1; IRE, inositol-requiring enzyme.

viviridae family, encodes the viral structural proteins Core, E1, E2, and p7, as well as six nonstructural proteins (8, 9). Two *N*-glycosylated envelope proteins E1 and E2 are exposed on the surface of the virus and are necessary for viral entry.

The aim of this study was to investigate whether the ERAD pathway is activated upon HCV infection and whether this affects the quality control of virus glycoproteins and virion production. We show that HCV infection triggers the ERAD pathway, possibly through IRE1-mediated splicing of XBP1. Moreover, EDEM1 and EDEM3, but not EDEM2, interact with HCV glycoproteins, resulting in increased ubiquitylation. EDEM1 knockdown and chemical inhibition of the ERAD pathway increases glycoprotein stability, as well as production of infectious virus particles, whereas overexpression of EDEM1 decreases virion production. These results provide insight into the mechanism by which HCV triggers the ERAD pathway and subsequently affects the quality control of virus glycoproteins and virus particle production.

EXPERIMENTAL PROCEDURES

Cell Culture and Chemicals—Human hepatoma cells HuH-7 and HuH-7.5.1 (a gift from Dr. F. V. Chisari (The Scripps Research Institute) (10) and human embryonic kidney cells 293T were cultured at 37 °C and 5% CO_2 in DMEM containing 10% FBS, 10 mM HEPES, 1 mM sodium pyruvate, nonessential minimum amino acids, 100 units/ml penicillin, and 100 μg/ml streptomycin. Tunicamycin (TM) was purchased from Sigma-Aldrich, and kifunensine (KIF) was purchased from Toronto Research Chemicals (Ontario, Canada).

Preparation of Virus Stock—HCV JFH-1 was generated by introducing *in vitro* transcribed RNA into HuH-7.5.1 cells by electroporation, and virus stocks were prepared by infecting at a multiplicity of infection (m.o.i.) of 0.01, as described previously (10). Infected cells were grown in culture medium containing 2% FBS, and supernatants were collected after multiple passages to get high titer virus. The supernatants were concentrated using a 500-kDa hollow fiber module (GE Healthcare) resulting in ~90% recovery of the virus. Focus-forming units were measured with an anti-HCV core antibody to determine virus titration (2H9, described below). Virus stocks containing 1×10^7 focus-forming units/ml were divided into small aliquots and stored at −80 °C until use. rAT strain of Japanese encephalitis virus (JEV) (11) was used to generate virus stock.

Plasmids—cDNAs of mouse EDEM1-HA, EDEM2, and EDEM3-HA, having 92, 93, and 91% amino acid homology with their human orthologs, respectively, were a kind gift from Drs. N. Hosokawa (Kyoto University) and K. Nagata (Kyoto Sangyo University). A HA tag was attached to the C terminus of EDEM2 by PCR, and sequencing analysis was performed to confirm the sequence. To generate pJFH/E1dTM-myc and pJFH/E2dTM-myc, HCV E1 encoding amino acids 170–352 and HCV E2 encoding amino acids 340–714 of JFH-1 polyprotein were amplified by PCR with forward primer and reverse primer containing NotI and XbaI restriction sites, respectively, and cloned into a NotI/XbaI site of the pEF1/Myc-His plasmid (Invitrogen). The pCAGC105E plasmid carrying PrM and E proteins of the rAT strain of JEV has been described (12). Plasmids carrying the firefly luciferase reporter gene under control of the intact promoter of GRP78 and GRP94 or the defective promoter lacking ERSE elements have been described (13) and were a kind gift from Dr. K. Mori (Kyoto University).

Antibodies—Rabbit polyclonal antibodies included anti-HA (Sigma-Aldrich), anti-HCV NS5A (14), anti-SEL1L (Sigma-Aldrich), anti-ubiquitin (MBL, Nagoya, Japan), and anti-JEV E antibodies. The mouse monoclonal antibodies were anti-HA (clone 16B12; Covance, Emeryville, CA), anti-HCV E2 (clone 8D10-3),[3] anti-β-actin (clone AC15; Sigma-Aldrich), anti-HCV core (clone 2H9) (15), and anti-Myc (clone 9E10; Santa Cruz Biotechnology, Santa Cruz, CA) antibodies. Anti-JEV antibodies have been described (16) and were a kind gift from Drs. C. K. Lim and T. Takasaki (National Institute of Infectious Diseases).

Analysis of XBP1 Splicing—Total RNA was extracted from cells using Isogen (Nippon Gene, Tokyo, Japan) following the manufacturer's protocol, and 2 μg of RNA was subjected to cDNA synthesis using oligo(dT) and Superscript III (Invitrogen). PCR was carried out using specific primers 5′-AAACAGAGTAGCAGCTCAGACTGC-3′ and 5′-GTATCTCTAAGACTAGGGGCTTGGTA-3′ for XBP1 and 5′-TCCTGTGGCATCCACGAAACT-3′ and 5′-GAAGCATTTGCGGTGGACGAT-3′ for β-actin to generate PCR fragments of 598 bp for unspliced XBP1, 572 bp for spliced XBP1, and 315 bp for β-actin. The following cycling conditions were used to amplify the genes: 1 cycle of 98 °C for 3 min, followed by 30 cycles of 98 °C for 20 s, 55 °C for 30 s, and 72 °C for 1 min, followed by a final extension of 72 °C for 10 min. The PCR product of XBP1 was further digested with PstI enzyme (New England Biolabs) and resolved on a 2% agarose gel prepared in TAE buffer. Unspliced XBP1 yielded two smaller fragments of 291 and 307 bp whereas spliced XBP1 stayed intact due to loss of the restriction site after splicing.

Gene Microarray Analysis—For microarray analysis, RNA was extracted from HuH-7.5.1 cells at 48 and 72 h after JFH-1 infection. Cells treated for 12 h with 5 μg/ml TM served as a positive control. Hybridization was performed on a 3D-Gene (see 3D-Gene web site) Human Oligonucleotide chip 25k (Toray Industries Inc., Tokyo, Japan). For efficient hybridization, this microarray chip has three dimensions and is constructed with a well between the probes and cylinder stems with 70-mer oligonucleotide probes on the top. Total RNA was labeled with Cy3 or Cy5 using the Amino Allyl MessageAMP II aRNA Amplification kit (Applied Biosystems). The Cy3- or Cy5-labeled aRNA pools were subjected to hybridization for 16 h using the supplier's protocol. Hybridization signals were scanned using a ScanArray Express Scanner (PerkinElmer Life Sciences) and processed by GenePixPro version 5.0 (Molecular Devices, Sunnyvale, CA). Detected signals for each gene were normalized using a global normalization method (Cy3/Cy5 ratio median = 1). Genes with Cy3/Cy5 normalized ratios $>\log_2 1.0$ or $<\log_2 -1.0$ were defined, respectively, as significantly up- or down-regulated genes.

Quantification of Cellular Gene Expression—Gene expression levels were measured using predesigned assay-on-demand (Applied Biosystems). RT-PCR amplification was performed

[3] D. Akazawa, N. Nakamura, and T. Wakita, unpublished data.

under the following conditions: 48 °C for 30 min, 95 °C for 10 min, 50 cycles of 95 °C for 15 s, and 60 °C for 1 min. Standard curves were constructed on a 1:5 serial dilution of the RNA template. The results were normalized to GAPDH mRNA levels.

Determination of Protein Stability—HuH-7 cells were infected with HCV JFH-1 at a m.o.i. of 2. Six hours after infection, the cells were either treated with KIF or transfected with EDEM1 siRNA. Forty hours later, culture medium was replaced with 100 μg/ml cycloheximide (CHX). Cells, including floating cells, were harvested at different time points after CHX addition, and immunoblotting was performed to determine the amount of HCV E2.

Plasmid Transfection and Immunoprecipitation—HuH-7 or 293T cells were seeded in 6-well cell culture plates at 3×10^5 cells/well and cultured overnight. Plasmid DNA was transfected into cells using TranIT-LT1 transfection reagent (Mirus, Madison, WI). Cells were harvested at 48 h after transfection, washed once with 1 ml of PBS, and lysed in 200 μl of lysis buffer (20 mM Tris-HCl, pH 7.4, 135 mM NaCl, 1% Triton X-100, and 10% glycerol supplemented with 50 mM NaF, 5 mM Na_3VO_4, and protease inhibitor mixture tablets (Roche Diagnostics). Cell lysates were sonicated at 4 °C for 10 min, incubated for 30 min at 4 °C, and centrifuged at 14,000 × *g* for 5 min at 4 °C. After preclearing for 2 h, the supernatants were immunoprecipitated overnight by rotating with 1.5 μl of anti-HA monoclonal antibody (16B12) or anti-HCV E2 monoclonal antibody (clone 8D10-3) at 4 °C. The immunocomplexes were then captured on protein G-agarose beads (Invitrogen) by rotation-incubation at 4 °C for 3 h. Beads were subsequently precipitated by centrifugation at 800 × *g* for 1 min and washed five times with lysis buffer. Finally, proteins bound to the beads were boiled in 40 μl of SDS sample buffer and subjected to SDS-PAGE.

Western Blotting—Proteins resolved by SDS-PAGE were transferred onto PVDF membranes (Immobilon; Millipore). After blocking in 2% skim milk, the membranes were probed with primary antibodies followed by exposure to peroxidase-conjugated secondary antibodies and visualization with an ECL Plus Western blotting detection system (GE Healthcare). The intensity of the bands was measured using a computerized imaging system (ImageJ software; National Institutes of Health).

Small Interfering RNA (siRNA) Transfection—HuH-7 cells were transfected with duplex siRNAs at a final concentration of 10 nM using Lipofectamine RNAiMAX (Invitrogen). Three siRNAs for each gene were examined for knock-down efficiency and cytotoxic effects. The siRNA with best performance was selected for further experiments. Target sequences of the siRNAs which exhibited the best knock-down efficiencies were as follows: EDEM1 (sense) 5′-CAUAUCCUCGGGUGAAUCUtt-3′, EDEM2 (sense) 5′-GAAUGUCUCAGAAUUCCAAtt-3′, EDEM3 (sense) 5′-CAUGAGACUACAAAUCUUAtt-3′, IRE1 (sense) 5′-GGACGUGAGCGACAGAAUAtt-3′. 5′-GGUGUCCUUACCAUACUAAtt-3′ served as a negative control. The lowercase letters denote overhanging deoxyribonucleotides.

Quantification of HCV Core and RNA—HCV core was quantified using an enzyme immunoassay (Ortho HCV antigen ELISA kit; Ortho Clinical Diagnostics, Tokyo, Japan). HCV RNA was quantified as described (17).

Statistical Analysis—Student's *t* test was employed to calculate the statistical significance of the results. $p < 0.05$ was considered significant.

RESULTS

HCV Infection Induces XBP1 mRNA Splicing and EDEM Expression—XBP1 plays a key role in activating the ERAD pathway, which mediates unfolded protein response in the ER. Under conditions of ER stress, XBP1 mRNA is processed by unconventional splicing and translated into functional XBP1, which in turn mediates transcriptional up-regulation of a variety of ER stress-dependent genes. The resultant activation of downstream pathways boosts the efficiency of ERAD, which coincides with elevated transcription of EDEMs. To validate our method for detecting activation of the ERAD pathway, we exposed HuH-7.5.1 cells to TM, which is a typical ER stress inducer, and performed an assay to quantify spliced XBP1 mRNA, as described under "Experimental Procedures," at different time points after treatment. The spliced form of XBP1 mRNA started accumulating within these cells as early as 2 h after exposure to TM (Fig. 1*A*), and levels remained elevated until at least 12 h after treatment. Quantitative RT-PCR showed that mRNA levels of EDEM1, EDEM2, and EDEM3 were elevated in TM-treated cells whereas ER ManI, which is not an ER stress-responsive gene, did not show any up-regulation (Fig. 1*B*). To examine involvement of the ERAD pathway in the HCV life cycle, we infected HuH-7.5.1 cells with JFH-1 at m.o.i. of 5 and analyzed XBP1 mRNA splicing and EDEM up-regulation. Upon infection, the fragment corresponding to spliced XBP1 mRNA, was detectable 8 h after infection, and the difference in splicing between mock- and HCV-infected cells became more pronounced at 48 h after infection and then persisted (Fig. 1*C*). Increased levels of XBP1 mRNA splicing were dependent on the m.o.i. (supplemental Fig. 1*A*), suggesting that expression of active XBP1 was induced by HCV infection. A small amount of spliced XBP1 was detected in mock-infected cells, presumably because of some intrinsic stress. A 3.1-fold increase in the level of EDEM1 mRNA was observed at 3–4 days after infection ($p < 0.05$). Increases in EDEM2 and EDEM3 mRNA levels were moderate and reached ~1.5-fold, whereas ER ManI mRNA exhibited no change after infection (Fig. 1*D*). Expression of EDEMs, particularly EDEM1, was up-regulated in accordance with HCV infection titers (supplemental Fig. 1*B*). Knocking down the IRE1 gene (Fig. 1*E*) effectively reversed the accumulation of spliced XBP1, as well as the transcriptional up-regulation of EDEM1 (Fig. 1*F*), thus confirming that HCV infection induces ERAD through the IRE1-XBP1 pathway.

To enable a comprehensive investigation of the transcriptional changes that occur, up- and down-regulation of the transcriptome was examined in HCV-infected cells and in TM-treated cells. The results were compared with those of mock-transfected cells at each time point. A range of genes involved in ER stress was found to be regulated in HCV-infected and in TM-treated cells (Fig. 2*A*). EDEM1 was signifi-

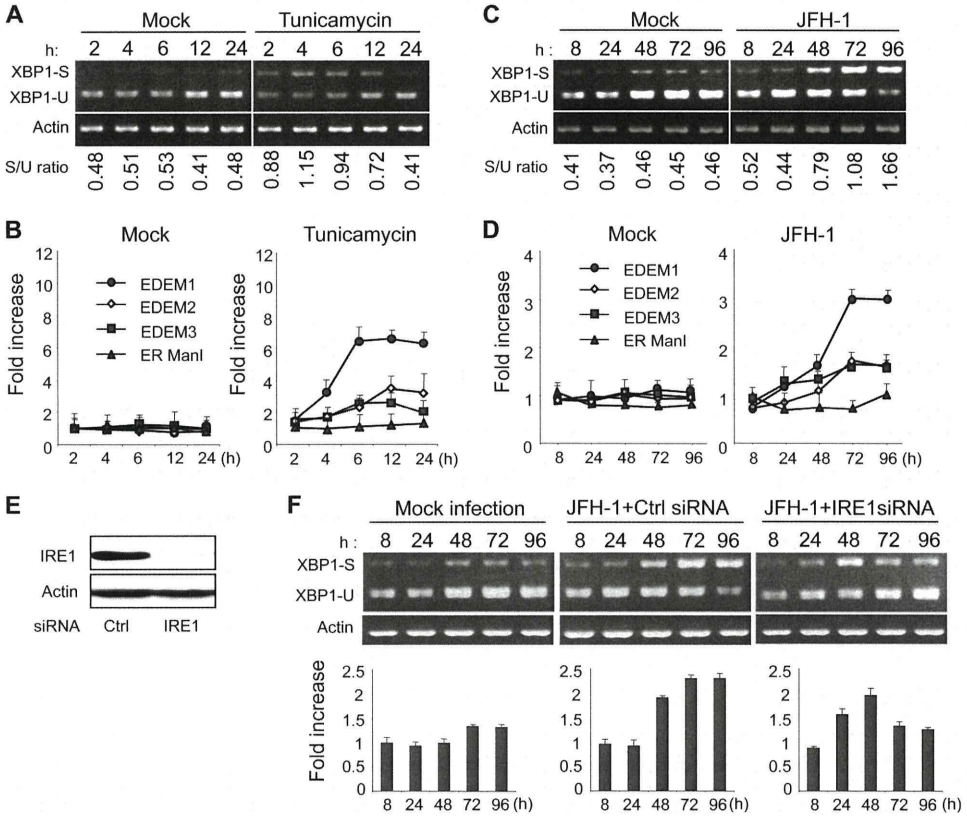

FIGURE 1. **Splicing of XBP1 mRNA and induction of ERAD gene expression in HCV JFH-1-infected cells.** *A*, splicing of XBP1 mRNA analyzed in mock- and TM (5 μg/ml)-treated HuH-7.5.1 cells at different time points after treatment. The *upper* and *lower bands* represent spliced and unspliced RNA, respectively. The *numbers* at the *bottom* of the *panel* indicate the density ratios of bands corresponding to spliced and unspliced XBP1. *B*, graphs showing the -fold induction of EDEM1, EDEM2, EDEM3, and ER Man1 mRNA in HuH-7.5.1 cells treated or untreated with TM. Data are normalized to GAPDH expression levels. The mean ± S.D. (*error bars*) of three independent experiments are shown. *C*, splicing of XBP1 mRNA analyzed in mock- and HCV JFH-1-infected HuH-7.5.1 cells (m.o.i. 5) at different time points after infection. *Numbers* at the *bottom* of the *panel* indicate the density ratios of bands corresponding to spliced and unspliced XBP1. *D*, real-time PCR analysis of EDEM1, EDEM2, EDEM3, and ER ManI mRNA induction in mock- and HCV-infected cells. Data are normalized to GAPDH expression. The mean ± S.D. of three independent experiments are shown. Note that a reduction in the level of GAPDH mRNA within infected cells was not observed until 96 h after infection when a slight decrease was observed. This led us to use GAPDH as a housekeeping gene in our experiments. *E*, Western blotting of IRE1 in cells transfected with mock or gene-specific siRNA of IRE1. *F*, splicing of XBP1 mRNA and induction of EDEM1 in HCV-infected cells after knocking down of the IRE1 gene. HuH-7.5.1 cells infected with JFH-1 at a m.o.i. of 5 were transfected with mock (*center*) or IRE1-specific siRNA (*right*) 48 h after infection, after which splicing of XBP1 (*upper*) and transcriptional up-regulation of EDEM1 (*lower*) were examined at the indicated time points after infection. The mean ± S.D. of two independent experiments are shown.

cantly up-regulated upon HCV infection, whereas expression levels of EDEM2 and EDEM3 remained unchanged. Although transcriptional changes caused by HCV infection in many of the genes listed are analogous to those that occur in cells treated with TM, up-regulation of two ER chaperone proteins, GRP78 and GRP94, was induced by TM treatment but not by HCV infection. This differential induction was confirmed by a reporter assay for GRP78 promoter and GRP94 promoter activities (Fig. 2*B*). These results are in agreement with a previously described finding that GRP78 and GRP94 are not responsive to HCV infection in hepatoma cells (18). It remains likely that HCV infection interferes with transcriptional activation of some ER chaperone proteins; however, the mechanism by which this occurs remains to be elucidated.

EDEMs Cause Ubiquitylation of HCV Glycoproteins and Enhance Their Degradation—Because EDEMs have been reported to enhance proteasomal degradation of ERAD substrates through direct binding, we investigated the interaction of EDEMs with HCV glycoproteins in 293T cells by co-transfecting the expression plasmids for E1dTM or E2dTM together with plasmids carrying either EDEM or ER ManI genes. Immunoprecipitation and immunoblotting demonstrated that each EDEM, but not ER ManI, was capable of interacting with E2 (Fig. 3*A*) and E1 (supplemental Fig. S2). HCV glycoproteins displayed enhanced mobility when co-expressed with EDEM1, EDEM3, or ER ManI, which could be due to the mannosidase activity of these proteins, which is lacking in EDEM2 (6). HCV primarily replicates in hepatocytes so we examined the interaction of EDEMs with E2dTM in HuH-7 cells as well, which yielded similar results (data not shown). E2dTM lacks the transmembrane domain, which could affect its folding and ER retention and thus modulate the ability of this protein to interact with EDEMs and ER ManI. Second, E1 and E2 glycoproteins assemble as noncovalent heterodimers to make functional complexes, which may alter the interaction of these proteins with EDEMs. To address these issues, we co-transfected HuH-7 cells with plasmids carrying full-length E1E2 glycoproteins together with plasmids carrying either EDEMs or ER ManI. Similar phenotypes were produced following transfection full-length E1E2 proteins (supplemental Fig. S3*A*), demonstrating that functional complexes of HCV glycoproteins bind with EDEMs. Recently, we have reported on the development of a

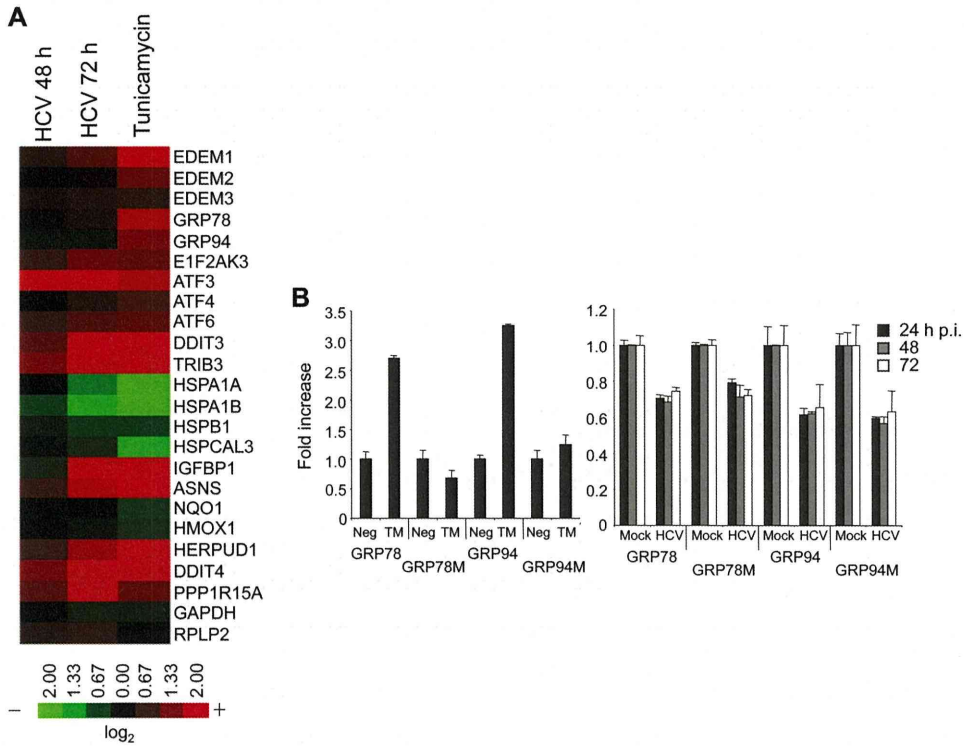

FIGURE 2. **Comprehensive analysis of ERAD gene expression in JFH-1-infected HuH-7.5.1 cells.** *A*, HuH-7.5.1 cells treated with TM (5 μg/ml) for 12 h or infected with JFH-1 for 48 and 72 h were subjected to microarray analysis, along with their negative controls. Expression of ER stress genes is shown as a heat map. *Red* and *green* indicate up- and down-regulation, respectively. Information on each gene shown is indicated on the 3D-Gene web site. *B*, GRP78 and GRP94 induction in TM-treated (*left*) and HCV-infected cells (*right*). GRP78M and GRP94M represent the defective promoters. The mean ± S.D. (*error bars*) of three independent experiments are shown.

packaging system of HCV subgenomic replicon sequences through the provision of viral core NS2 proteins in *trans* (19). Transcomplementation with core NS2 proteins resulted in successful packaging of the viral sequences; therefore, plasmids carrying these proteins are a valid construct by which to examine the interaction of envelope proteins with ERAD machinery. Thus, we performed an immunoprecipitation assay of HuH-7 cells co-transfected with core NS2 and EDEMs. In agreement with our previous results, EDEMs, but not ER ManI, were observed to bind to HCV E2 protein (supplemental Fig. S3*B*). To examine the functional importance of this interaction, we analyzed the ubiquitylation of HCV E2 protein in cells co-transfected with HCV E2 and EDEM proteins. An immunoprecipitation assay revealed that overexpression of EDEM1 and EDEM3, but not of EDEM2 and ER ManI, dramatically increased the ubiquitylation of HCV glycoprotein (Fig. 3*B*). In mammals, the ER membrane ubiquitin-ligase complex involved in the dislocation of ERAD substrates, and their ubiquitylation contains the ER membrane adaptor SEL1L. It has recently been shown that SEL1L interacts with EDEM1 in cells and functions as a cargo receptor for ERAD substrates (20); however, it is unknown whether SEL1L interacts with other EDEMs. We therefore assessed whether SEL1L interacts with EDEM1, EDEM2, EDEM3, and ER ManI in cells (Fig. 3*C*). Interestingly, endogenous SEL1L co-precipitated with EDEM1 and EDEM3, whereas little to no interaction was observed with EDEM2 and ER ManI. Collectively, it is likely that, although all EDEMs can recognize HCV E1 and E2, EDEM1 and EDEM3 are involved in the ubiquitylation of HCV glycoproteins by delivering them to SEL1L-containing ubiquitin-ligase complexes. To investigate further the role of EDEMs in quality control of HCV glycoproteins, we measured the steady-state level of HCV E2 protein after EDEM knockdown. Transfection of HCV-infected cells with siRNAs against EDEM1, EDEM2, or EDEM3 caused a 60–80% reduction in mRNA levels of the respective genes (Fig. 3*D*) with no cytotoxic effects observed (data not shown). Immunoblotting showed a considerable increase in the steady-state level of viral E2 in EDEM1 siRNA-treated cells (Fig. 3*D*). We subsequently examined the turnover of E2 in cells with and without EDEM1 knockdown. In CHX half-life experiments, E2 protein was moderately unstable in control-infected cells, presumably via proteasomal degradation (Fig. 3*E*). Treatment with MG132, a proteasome inhibitor, blocked its destabilization (data not shown). In contrast, E2 was completely stable in EDEM1-knockdown cells during the chase period of time tested (Fig. 3*E*). Together, these results strongly suggest that EDEM1 and EDEM3, particularly EDEM1, are involved in the post-translational control of HCV glycoproteins.

Involvement of EDEM1 in the Production of Infectious HCV—Given the involvement of EDEMs in the turnover of HCV glycoproteins, we investigated whether EDEMs affect the replication and production of infectious virus particles. EDEMs were knocked down in HCV-infected HuH-7 cells by siRNA transfection, and the production of infectious particles was then monitored by measuring the extracellular infectivity titer. Knocking down of EDEM1 and EDEM3 in the infected cells resulted in ~3.1-fold ($p < 0.05$) and ~2.3-fold increases in virus production, respectively, compared with control cells. No effect